

## Mapping soil salinity in irrigated land using optical remote sensing data

Rachid Lhissou <sup>a</sup>, Abderrazak El Harti <sup>a,\*</sup>, Karem Chokmani <sup>b</sup>

<sup>a</sup> Team of Remote Sensing and GIS Applied to Geosciences and Environment, Faculty of Sciences and Techniques, Beni Mellal, Morocco

<sup>b</sup> Institut National de la Recherche Scientifique, Centre- Eau, Terre & Environnement 490, Canada

### Abstract

Soil salinity caused by natural or human-induced processes is certainly a severe environmental problem that already affects 400 million hectares and seriously threatens an equivalent surface. Salinization causes negative effects on the ground; it affects agricultural production, infrastructure, water resources and biodiversity. In semi-arid and arid areas, 21% of irrigated lands suffer from waterlogging, salinity and/or sodicity that reduce their yields. 77 million hectares are saline soils induced by human activity, including 58% in the irrigated areas. In the irrigated perimeter of Tadla plain (central Morocco), the increased use of saline groundwater and surface water, coupled with agricultural intensification leads to the deterioration of soil quality. Experimental methods for monitoring soil salinity by direct measurements in situ are very demanding of time and resources, and also very limited in terms of spatial coverage. Several studies have described the usefulness of remote sensing for mapping salinity by its synoptic coverage and the sensitivity of the electromagnetic signal to surface soil parameters. In this study, we used an image of the TM Landsat sensor and field measurements of electrical conductivity (EC), the correlation between the image data and field measurements allowed us to develop a semi-empirical model allowing the mapping of soil salinity in the irrigated perimeter of Tadla plain. The validation of this model by the ground truth provides a correlation coefficient  $r^2 = 0.90$ . Map obtained from this model allows the identification of different salinization classes in the study area.

### Article Info

Received : 01.05.2014

Accepted : 14.10.2014

**Keywords:** Soil salinity, Electric conductivity, spectral indices, principle component analysis

© 2014 Federation of Eurasian Soil Science Societies. All rights reserved

### Introduction

Soil salinization is the process of salts accumulation in the soil surface and in the root zone which causes harmful effects on plants and soil; it follows a decrease in yields, ultimately, soil sterilization. It reduces the area of farmland land 1 to 2% per year and continues to increase (FAO, 2002). In some countries, salinization may even threaten the national economy. This is particularly the problem of Argentina, Egypt, India, Iraq, Pakistan, Syria and Iran (Rhoades and Corwin, 1990). Soil salinization is characterized by its evolution in both time and space (Abbas et al., 2013). Therefore, the use of traditional methods (laboratory analysis, field survey) for its monitoring is insufficient and unsuited to the rate of evolution of this phenomenon and is demanding high costs, contrariwise to the optical satellite imagery that can be a powerful tool for mapping and continuous monitoring of the progression of this phenomenon by its synoptic coverage and the sensitivity of the electromagnetic signal to soil parameters at the first centimeters of the

\* Corresponding author.

Team of Remote Sensing and GIS Applied to Geosciences and Environment, Faculty of Sciences and Techniques, PO BOX. 523 Beni Mellal, Morocco

Tel.: +212523485112

ISSN: 2147-4249

E-mail address: [a.elharti@usms.ma](mailto:a.elharti@usms.ma)

surface layer, such as the dielectric constant that is directly related to the salt content of the soil (Farifteh et al., 2006; Metternicht and Zinck, 2003; Mougenot and Pouget, 1993).

According to the literature, the mapping of salinity risk has been the subject of several research projects operated with different types of multispectral remote sensing data. Abbas et al., (2013) and Khan et al. (2001) tested several indices namely the index of brightness (BI), the Normalized Difference Salinity Index (NDSI) and Salinity Index (SI). In the Norway Indian Project (Indo-Dutch Network Project, 2003), three salinity indices have been proposed; SI-1, SI-2 and SI-3. Al-Khair (2003) demonstrated the usefulness of the salinity index-SI using ASTER (Advanced Spaceborne Thermal Emission and Reflection Radiometer) sensor data in mapping salinity of irrigated farmland in Syria. Jenson (2007) cited that Dwivedi (1996) used principal component analysis; he argues that CP1 and CP2 can characterize soil salinity unlike other components. Bannari et al. (2008) proposed two indices: Soils and Salinity Sodicity Indices (SSSI SSSI-1 and-2) based on the SWIR spectral bands of ALI sensor (Advanced Land Imager). Douaoui et al. (2006) proposed three indices of salinity for the characterization of soil salinity in semi-arid climate.

The aim of this paper is the mapping of soil salinity in the irrigated perimeter of Tadla plain by developing a semi-empirical model based on optical remote sensing data and field measurements of electrical conductivity (EC). In our case, we assessed several spectral transformations such as spectral indices previously cited, and principal components derived from Landsat TM satellite image for estimating soil salinity.

## Material and Methods

### Study area and data used

The study area site is the agricultural plain of Tadla in Tadla-Azilal Region in central Morocco, located between  $6^{\circ}51'49.1''$  W and  $6^{\circ}30' 46.85''$  W longitude and  $32^{\circ}19'04.39''$  N and  $32^{\circ}32'04.41''$  N latitude (Figure 1). It is irrigated by water collected by the Ahmed El-Hansali dam. The soil of this site is characterized by secondary salinization induced by irrigation. As for the climate, it is of a continental and mediterranean type, characterized by a wet season from October to April and a dry season that lasts from May to September. The absolute temperatures recorded over the past 40 years vary between  $-6^{\circ}$  and  $46^{\circ}$  C. The annual average of rainfall recorded between 1971 and 2010 varied between 127 and 638 mm (Bachaoui et al., 2014). The Landsat TM image was acquired over the plain of Tadla on 14 September 2011 simultaneously with the field measurements campaign. These are used to calibrate and validate the developed model.

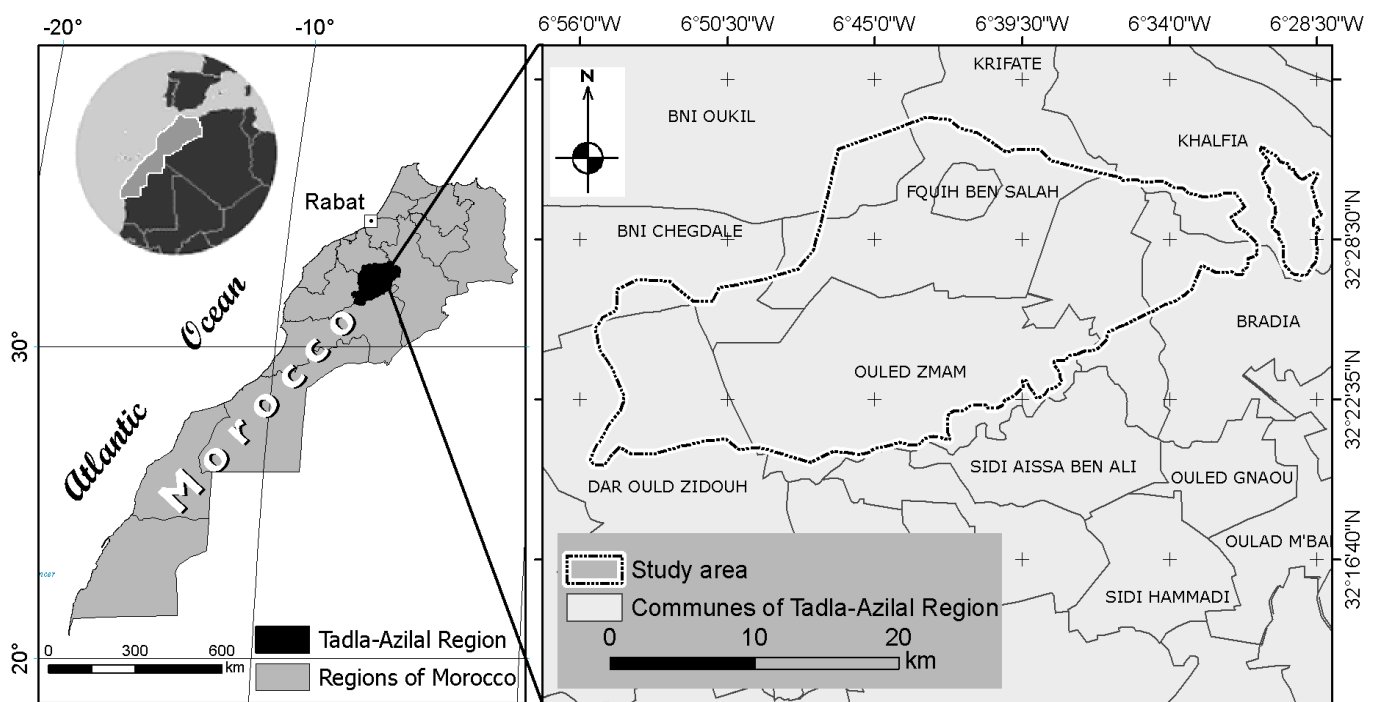


Figure 1. Geographical location of the irrigated perimeter of Tadla

## Methodology

The methodology adopted in this research is illustrated in Figure 2. First of all, the radiometric and atmospheric corrections of errors due to the sensor and atmospheric effects were made. Second of all, the spectral indices of soil salinity, the Normalized Difference Vegetation Index (NDVI) and the principal components were calculated. Finally, all derived data were compared with field measurements of soil EC to extract an EC estimation model allowing soil salinity mapping. It proved essential to remove vegetation because of the importance of its cover. The optical imaging was used to map vegetation by calculating the NDVI. Using this image, we also masked the built-up area in the study site.

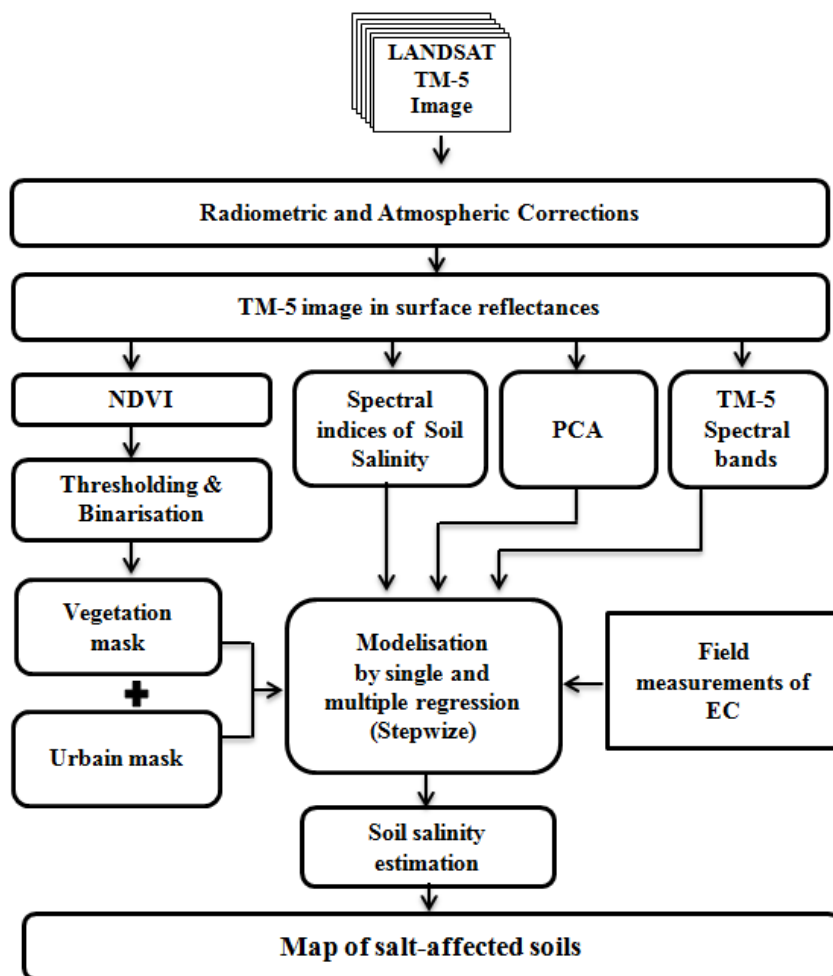


Figure 2. Methodology flowchart

## Field measurements of electrical conductivity

Soil samples were collected during the field survey (Figure 3) and their electrical conductivity was measured in the laboratory using physicochemical analysis. EC is often used to measure soil and water salinity. It is expressed in deciSiemens per meter (dS/m). Thus, we used the EC to classify the level of soil salinity as follows: non-saline soil :  $0 < dS/m < 2$  ; Slight saline soil:  $2 < dS/m < 4$  ; Moderate saline soil:  $4 < dS/m < 6$ , Strongly saline soil:  $6 < dS/m < 8$  and Heavy saline soil:  $> 8$  [14]. Before the interpolating of field measurements to obtain a EC map, we studied the spatial structure of the variable using a variogram using the ArcGIS10.0

software. Finally, it was found that the variable is spatialisable. After several tests of deterministic and geostatistical methods, the universal kriging provided the best model.

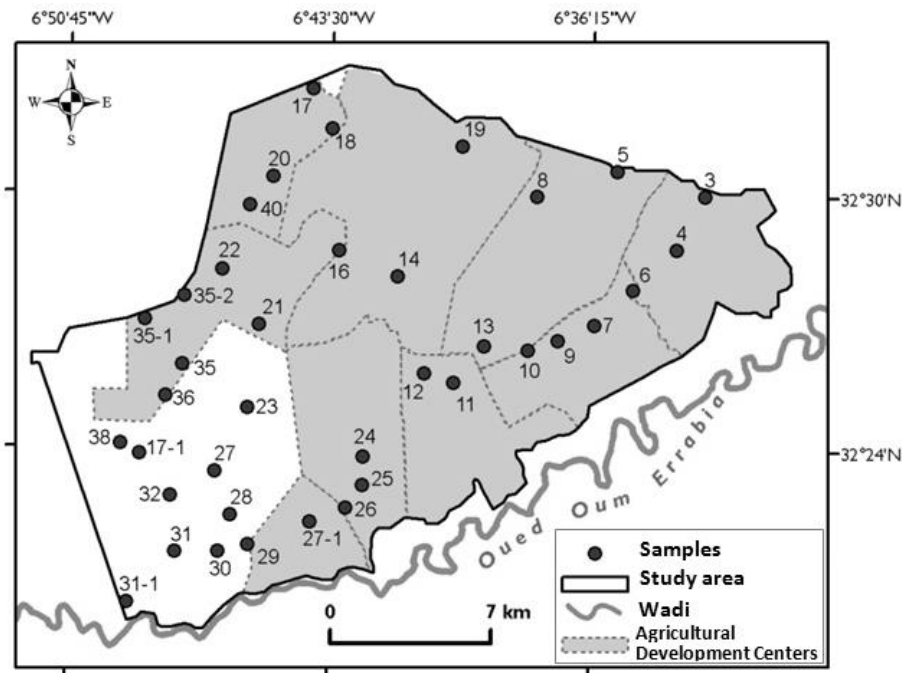


Figure 3. Location of sampling points

### Image data pre-processing

The radiometric calibration of the sensor is the operation that leads to establish the relationship between the measured physical amounts at the sensor field of view, the radiation flow reflected by the earth-atmosphere system, and the apparent digital number  $DN(\lambda)$  at the exit of the instrument towards the reception stations (Chen, 1997). It is a critical step that consists of correcting the radiometric sensor drift to extract reliable and precise information from the image. The raw data from the  $DN(\lambda)$  was converted into spectral radiance  $L(\lambda)$  using sensor's the calibration coefficients (gain and offset). The  $L(\lambda)$  was calculated using the following equation:

$$L(\lambda) = G(\lambda) \cdot DN(\lambda) + O(\lambda) \tag{1}$$

$DN(\lambda)$  : Digital number at the sensor's aperture;

$L(\lambda)$  : Spectral radiance at the sensor's aperture [W/(m<sup>2</sup> sr μm)];

$O(\lambda)$  : Offset;

$G(\lambda)$  : Gain;

As for the atmospheric effects, it is dominated by the absorption caused by the gases (water vapor, carbon dioxide, and ozone) and the diffusion produced by the aerosols and the molecules (Richards, 1993; Burgess et al., 1995). In this research we used the FLAASH atmospheric correction model to obtain surface reflectance. This model uses the look-up-tables with five dimensions (Staenz et al., 2002), are the wavelength, the pixel position, the water vapor in the atmosphere, the terrain elevation and the optical depth of atmosphere. FLAASH starts from a standard equation for spectral radiance  $L(\lambda)$  at a sensor pixel to determine the surface reflectance following the equation 2. Table 1 present input parameters used in FLAASH model.

$$L(\lambda) = \frac{A\rho}{1 - \rho_e S} + \frac{B\rho_e}{1 - \rho_e S} + L_a(\lambda) \tag{2}$$

Where:

$\rho$  : Pixel surface reflectance;

$\rho_e$  : Average surface reflectance for the pixel and a surrounding region;

$S$  : Spherical albedo of the atmosphere;

$L_a(\lambda)$  : Radiance back scattered by the atmosphere;

$A$  and  $B$ : Coefficients that depend on atmospheric and geometric conditions but not on the surface.

Table 1. Input parameters used in FLAASH model

Parameters	values
Ground elevation (km)	1.5
Sensor altitude (km)	705
Sensor type	Thematic Mapper (TM5)
Acquisition date	9/14/2011
Decimal hour	10,50
Localisation	6°19'7,68"W 31°44'27,24"N
Atmospheric model	Mid-Latitude summer
Aerosol model	Rural model
Visibility (km)	50

### Principal component analysis (PCA)

PCA is a mathematical transformation based on the analysis of the covariance or the correlation matrix of several spectral bands (Bonn and Rochon, 1992; Caloz and Collet, 2001). It reorganizes the data so that they are no longer correlated and redundant (Frans and Schowengerdt, 1997). Theoretically, it offers an interesting approach to deal with the identification of soil salinity and changes detection. The stability of the brightness of PC1 and PC2 allows the separation of non-saline soils and saline, which could not be detected by PC3 and PC4 (Metternich and Zinck, 2003; Jenson, 2007). Only PC1 and PC2 were considered in this research to analyze their potential to detect different salt levels in soils.

## Results and Discussion

### Assessment of spectral indices

The various indices calculated were evaluated; Table 2 shows the result of evaluation. The index that gave the best correlation is the SI index with  $R^2 = 0.6$  and  $RMSE = 0.24$ . In general, the spectral indices based on the visible spectral bands are more sensitive to changes of the EC against those based on near-infrared and mid-infrared with the exception of the index SSSI-1.

Table 2 : Correlations between the spectral indices of salinity and soil EC.

Spectral indices	$R^2$	RMSE	Equation	Source
BI	0,475	0,93	$\sqrt{TM3^2 + TM4^2}$	Khan et al. (2001)
NDSI	0,01	1,79	$(TM3 - TM4) / (TM3 + TM4)$	Khan et al. (2001)
SI	0,68	0,24	$\sqrt{TM1 * TM3}$	Khan et al. (2001)
ASTER-SI	0,067	1,45	$(TM5 - TM7) / (TM5 + TM7)$	Al-Khaier (2003)
SI-1	0,06	1,99	$(TM5) / (TM7)$	IDNP (2002)
SI-2	0,045	0,87	$(ALI4 - TM3) / (ALI4 + TM3)$	IDNP (2002)
SSSI-1	0,501	0,54	$(TM5 - TM7)$	Bannari et al. (2007)
SSSI-2	0,385	0,69	$(TM5 * TM7 - TM7 * TM7) / TM5$	Bannari et al. (2007)
SI-1(2)	0,555	0,24	$\frac{\sqrt{G * R}}{\sqrt{G^2 + R^2 + NIR^2}}$	Douaoui et al. (2006)
SI-2(2)	0,493	0,98	$\frac{\sqrt{G^2 + R^2 + NIR^2}}{\sqrt{G^2 + R^2}}$	Douaoui et al. (2006)
SI-3(2)	0,53	0,92	$\sqrt{G^2 + R^2}$	Douaoui et al. (2006)

### Modelling soil salinity and validation results

Firstly, the data were calibrated by pixel and by locally in a window of size 3x3 pixels. Then, the calibration was made using the territory segmentation based on the EC classes obtained by the field measurements interpolation. This latter approach provides a more accurate estimation than the first two approaches, which

is due to the high variability of salinity per unit of distance and the large pixel size of data (30 meters). Table 3 presents the best models for the EC estimation obtained by the three calibration methods; by pixel, window of 3x3 pixels and EC classes.

Table 3. Optimal models and their performance parameters

Calibration	By pixel	By window (3x3)	By classes
Estimated EC	$\text{Exp}((-0,022)*(\text{CP}2)+0,692)$	$\text{exp}((7,423)*(\text{SI})+1,802)$	$-0,142*(\text{SI})+2,475$
R <sup>2</sup>	0,64	0,688	0,908
RMSE	0,319	0,310	0,293

### Soil salinity mapping using the developed model

Cross-validation showed that the model calibrated by classes and based on the SI spectral index model is the most efficient in estimating the electrical conductivity, presenting a higher coefficient of determination  $R^2 = 0.904$  (Figure 4a). In addition, the validation of this model by external measurements of EC provided by the Office Régionale de Mise en Valeur Agricole of Tadla (ORMVAT) presented a  $R^2 = 0.6$  (Figure 4b). Thereafter, the image obtained by this model has been classified to produce the salinity map (Figure 4c).

The most affected areas by the high salinity are located in the hydraulically downgradient (Figure 4c, zone 2 and 3), following a recycling of salty groundwater by pumping. The results obtained show an EC from 3.00 to 9.00 dS / m in the affected areas. From the comparison between the obtained soil salinity map, the groundwater level map and the map of the groundwater salinity, we note that the soil salinity is very important in zones 2 and 3 where the level of the groundwater is very close to the surface and also the groundwater salinity is high contrariwise to zone 1 where soil salinity is low (Figure 4c, zone 1).

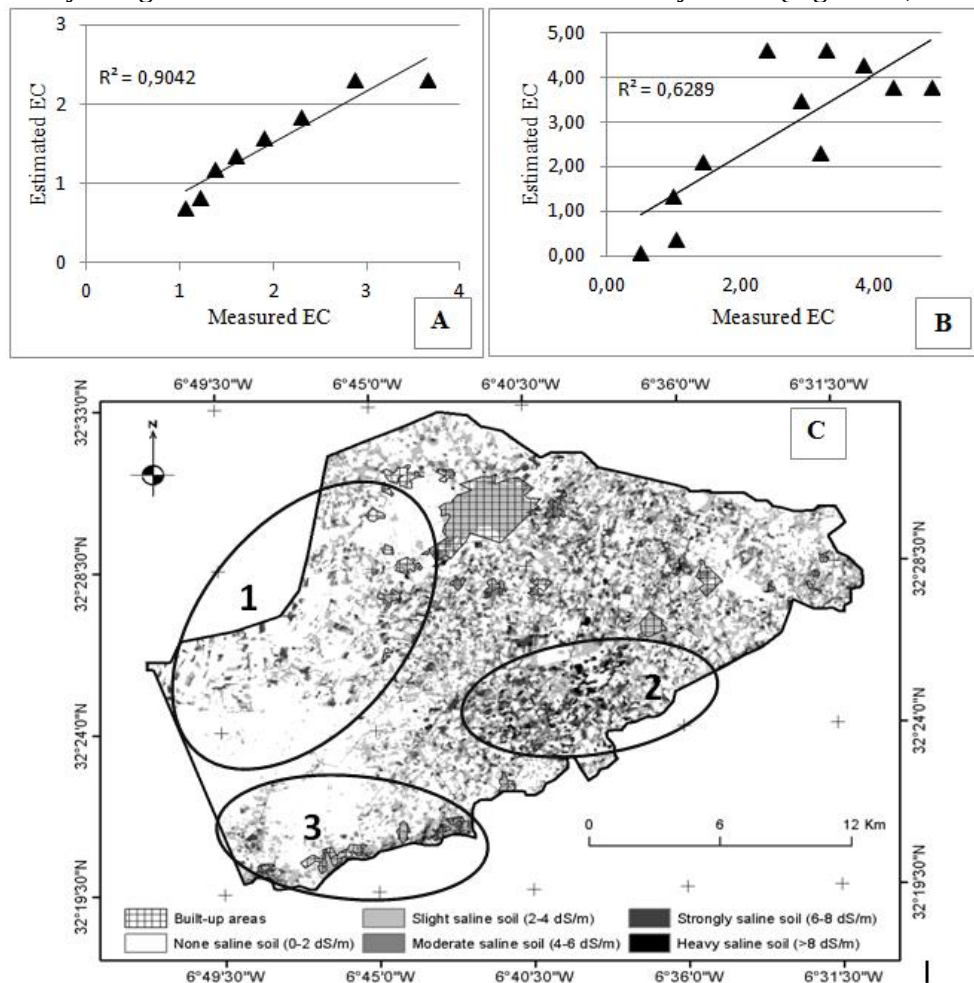


Figure 4. Model based on SI index for estimating and mapping soil salinity; A: Cross-validation results, B: Validation by others samples, C: Final soil salinity map of the study area

## Conclusion

The results of this paper show that soil salinity could be estimated well using spectral indices as a good auxiliary variable in the spatial estimation and mapping salinity in irrigated land. For this purpose, the indices based on the visible spectral bands are more sensitive to the soil salinity and the SI index has a better correlation with soil salinity in our region than the others. The Stepwise regression allowed finding the most correlated parameters with soil salinity. Finally, Calibration based on the largest unit of aggregation gives a more accurate model, because it reduces the effects of the high soil salinity variability. Otherwise, we need to expand the mesh of soil samples to get the best estimates.

## Acknowledgements

The authors would like to acknowledge the Office Régional de Mise en Valeur Agricole of Tadla (ORMVAT) for their assistance during the field works and providing several data. We gratefully acknowledge the AUF (Agence Universitaire de la Francophonie) for financial support to this collaboration.

## References

- Abbas, A., Khan, S., Hussain, N., Hanjra, M.A., Akbar, S., 2013. Characterizing soil salinity in irrigated agriculture using a remote sensing approach. *Physics and Chemistry of Earth, Parts A/B/C*, 55-57, 43-52.
- Al-khaier, F., 2003. Soil Salinity detection using satellite Remote Sensing. International Institute for Geo-Information Science and Earth Observation, Enschede, The Netherlands. 61 p.
- Bachaoui, B., Bachaoui, E., Maimouni, S., Lhissou, R., El Harti, A., El Ghmari, A., 2014. The use of spectral and geomorphometric data for water erosion mapping in El Ksiba region in the central High Atlas Mountains of Morocco. *Applied Geomatics* 6(3), 159-169.
- Bannari, A., Guedon, A.M., El-Harti, A., Cherkaoui, F.Z., El-Ghmari, A., 2008. Characterization of slightly and moderately saline and sodic soils in irrigated agricultural land using simulated data of advanced land imaging (EO-1) sensor. *Communications in Soil Science and Plant Analysis* 39 (19), 2795-2811
- Bonn, F., Rochon, G. 1992. Précis de télédétection. Vol. 1 : Principes et méthodes. Presses de l'Université du Québec et l'AUPELF, Sainte-Foy et Montréal, 485 p.
- Burgess, D. W., Lewis, P., Muller, J. P., 1995. Topographic Effects in AVHRR NDVI Data. *Remote Sensing of Environment*, 45, 223-232.
- Caloz, R., Collet, C., 2001. Traitements numériques d'images de télédétection. Presses de l'université du Québec/AUPELF, Québec, 380p.
- Chen, H. S., 1997. Remote Sensing Calibration Systems: An Introduction. DEEPAK.
- Douaoui, A.K., Herve', N., Walter, C., 2006. Detecting salinity hazards within a semiarid context by means of combining soil and remotesensing data. *Geodema*, 134, 217-230.
- FAO, 2002. Le The salt of the earth: hazardous for food production. Word Food Summit. Five years later. 10-13 June 2012. Available at: <http://www.fao.org/worldfoodsummit/english/newsroom/focus/focus1.htm>
- Farifteh, J., Farshad, A., George, R.J., 2006. Assessing salt-affected soils using remote sensing, solute modelling, and geophysics. *Geoderma* 130 (3-4), 191-206.
- Frans E.P., Schowengerdt, R.A. 1997. Spatial-Spectral Unmixing Using the sensor PSF, Proc. SPIE, Vol. 3118, Imaging Spectrometry III, San Diego, CA.
- IDNP, 2003. Indo-Dutch Network Project: A Methodology for Identification of Waterlogging and Soil Salinity Conditions Using Remote Sensing. Central Soil Salinity Research Institute, Karnal, India, 78 pages.
- Jenson, J., 2007. Remote Sensing of the environnement, an earth resource perspective. 2ème edition. 591 p.
- Khan, N.M., Rastoskuev, V.V., Shalina E.V., Sato, Y., 2001. Mapping salt affected soils using remote sensing indicators: A simple approach with the use of GIS IDRISI. In: Proceedings of the 22nd Asian Conference on Remote Sensing. 5 - 9 November 2001, Singapore.
- Metternich, G.I., Zinck, J.A., 2003. Remote sensing of soil salinity: potential and constraints. *Remote Sensing of Environment* 85, 1-20.
- Mougenot, B., Pouget, M., 1993. Remote sensing of salt-affected soil. *Remote Sensing Reviews* 7, 241-259.
- Rhoades, J.D., Corwin, D.L., 1990. Soil electrical conductivity: effects of soil properties and application to soil salinity appraisal. *Communication in Soil Science and Plant Analyses* 21: 836-860.
- Richards, J. A., 1993. Remote Sensing Digital Image Analysis (2nd Edition). Springer-Verlag, New York, 340 p.
- Richards, L.A., 1954. Diagnosis and improvements of saline and alkali soils. U.S. Salinity Laboratory. US Dept. of Agronomy Handbook 60, 160 p.
- Staez, K., Secker, J., Gao, B.C., Davis, C., Nadeau, C., 2002. Radiative transfer codes applied to hyperspectral data for the retrieval of surface reflectance. *ISPRS Journal of Photogrammetric Engineering and Remote Sensing*, 57(3), 194-203.